

Laboratory and field studies of colloidal iron oxide dissolution as mediated by phagotrophy and photolysis

K. Barbeau¹ and J. W. Moffett²

Department of Marine Chemistry and Geochemistry, Woods Hole Oceanographic Institution, Woods Hole, Massachusetts 02453

Abstract

In a previous work, we have employed colloidal ferrihydrite impregnated with an inert radiotracer to probe the mechanistic of iron redox cycling in seawater via phagotrophic and photochemical processes. This paper reports further studies using the inert tracer technique, directed towards obtaining a more quantitative sense of the importance of phagotrophy relative to photolysis as a pathway for the production of bioavailable iron in oxygenated seawater. Our results indicate a maximal (i.e., near-surface at noon) rate of 12% per day for the photochemically-mediated dissolution of colloidal ferrihydrite. Protozoan-mediated dissolution of the same iron oxide phase proceeds at a rate ranging from 1–6% per day, depending on grazing turnover rates. Thus, while photolysis should dominate the redox cycling of refractory iron solids in near-surface waters under bright daytime conditions, phagotrophy is likely to be a more important process overall when the entire euphotic zone is considered on a time-averaged basis.

Since the first evidence for iron limitation of phytoplankton production in high nutrient, low-chlorophyll regions of the world's oceans (Martin and Fitzwater 1988; Martin and Gordon 1988), the seawater chemistry of iron and its relationship to phytoplankton have been the subject of intense research by a number of groups (*for review see* Wells et al. 1995; Price and Morel 1998). At this stage, a decade since Martin's pioneering work in the subarctic North Pacific, there seems little doubt that iron plays a pivotal role in ecosystem structure and function in several oceanic regions (e.g. Martin et al. 1994; Coale et al. 1996; de Baar et al. 1990; Landry et al. 1997; Hutchins and Bruland 1998).

Mechanisms that mediate the conversion of iron from the refractory pool to the labile, bioavailable pool in oceanic surface waters are important parameters in iron biogeochemistry. To date, several processes have been proposed to contribute to the maintenance of the available iron pool, including photoreduction, ligand complexation, enzymatic reactions, and thermal reactions. Of these, photoreduction has been most thoroughly characterized in terms of its ability to generate an increase in iron reactivity in natural waters, and it is believed to be an important pathway for the formation of labile iron species (e.g., Waite and Morel 1984; Wells and Mayer 1991; Johnson et al. 1994).

In a previous work, using colloidal ferrihydrite as a model refractory phase, we have demonstrated that the grazing ac-

tivity of heterotrophic (phagotrophic) protists represents an additional mechanism for the production of reactive iron from nonbioavailable forms due to chemical reactions that take place within the acidic, reducing microenvironment of the phagotrophic food vacuole (Barbeau et al. 1996; Barbeau and Moffett 1998). Our estimates indicate that the maximal noon-time near-surface rate of iron photolysis exceeds the rate of protozoan-mediated iron reactions by approximately a factor of ten. However, when the maximal photoreduction rate is integrated temporally and spatially over the euphotic zone, it decreases by about an order of magnitude due to the effects of light attenuation with depth and diurnal variations in light intensity (Johnson et al. 1994). Relative to photoreduction, the rate of grazer-mediated processes in the upper water column changes much less with depth and over time. Thus, when integrated rates are considered, photoreduction and phagotrophy may ultimately be of similar magnitude in terms of their impact on iron speciation.

In this study, a novel tracer methodology was used to follow the reactions of refractory iron in seawater as mediated by both photochemistry and protozoan grazing. This method is based on the use of colloidal ferrihydrite uniformly impregnated with the radioisotope ¹³³Ba as a model phase for nonbioavailable iron. In seawater, dissolution of the iron oxide results in release of ¹³³Ba to the dissolved phase, where it accumulates due to the low biological and surface reactivity of Ba (e.g., Li et al. 1984; Fisher et al. 1991). The release and accumulation of ¹³³Ba in seawater is quantitatively related to the extent of dissolution of the ferrihydrite carrier phase, even for kinetically slow reactions and regardless of the fate of iron itself in the system (Barbeau and Moffett 1998).

This technique enables the study of photochemical and grazing effects on the same model iron oxide phase, under conditions relevant to natural waters. The experimental results described here not only provide some insight into how iron redox reactions in seawater are mediated by photolysis and phagotrophy, but also enable a more quantitative assessment of the relative importance of these two processes as influences on iron speciation in surface waters.

¹ Present address: Department of Chemistry and Biochemistry, University of California, Santa Barbara, California 93106.

² Corresponding author (e-mail: jmoffet@whoi.edu).

Acknowledgments

We thank Phoebe Lam for her assistance with the photochemical studies, and Oliver Zafiriou for use of the Hg/Xe lamp. We thank Dave Caron for assistance and advice on all aspects of this project, particularly the grazing field studies. This manuscript was substantially improved by the comments of two anonymous reviewers. This work was financially supported by a Department of Defense ONR-NDSEG Graduate Fellowship, Office of Naval Research AASERT Award (N00014-94-1-0711), and the National Science Foundation EGB Program (OCE-9523910). Contribution number 10144 from the Woods Hole Oceanographic Institution.

Table 1. Photochemistry in natural waters. Percentage of dissolved ^{133}Ba produced in 1-h Hg/Xe lamp irradiations of ^{133}Ba -ferrihydrite in various water types. Values shown for percent ^{133}Ba are the average and standard deviation of replicates. Samples above the dotted line were run on the same day, with the same batch of colloidal ferrihydrite. Samples below the line were run 2 days later, with a different batch.

Sample	Absorbance			Dark control % ^{133}Ba <0.05 μm	Irradiated % ^{133}Ba <0.05 μm	Rate of dissolved ^{133}Ba release \dagger
	(AU)*	pH	Salinity (ppt)			
VSW \ddagger	0.20	8	31	3.0 \pm 0.4	4.9 \pm 0.4	0.019 \pm 0.004 h $^{-1}$
SSW \S	0.03	8	35	3.1 \pm 0.1	5.3 \pm 1	0.022 \pm 0.01 h $^{-1}$
WB \parallel	0.34	8	24.2	2.9 \pm 0.1	5.8 \pm 0.1	0.029 \pm 0.001 h $^{-1}$
Estuary $\#$	0.60	7.6	15.4	2.2 \pm 0.9	4.5 \pm 0.9	0.023 \pm 0.009 h $^{-1}$
Salt Pond	0.78	6.0	1.1	3.0 \pm 0.4	7.6 \pm 3	0.046 \pm 0.03 h $^{-1}$

* Absorbance values at 300 nm, relative to Milli-Q water blank.

\dagger ^{133}Ba release rates are derived from the difference in percentage of dissolved ^{133}Ba between irradiated samples and dark controls.

\ddagger Vineyard Sound seawater.

\S Sargasso seawater.

\parallel Waquoit Bay water.

$\#$ 50/50 solution of Vineyard Sound seawater and Salt Pond water.

Methods

^{133}Ba -impregnated ferrihydrite—Details of the synthesis of ^{133}Ba -impregnated colloidal ferrihydrite as well as the theory and initial testing of the method have already been published elsewhere (Barbeau and Moffett 1998). The ferrihydrite is synthesized by neutralization of a mM ferric salt solution in the presence of μM concentrations of ^{133}Ba and trace amounts of ^{59}Fe . The initial product of this basic hydrolysis is a 2-line ferrihydrite, which is subsequently heated briefly at 90°C to obtain a phase that is still subcrystalline and similar in reactivity to a 6-line ferrihydrite. In order to rinse away excess ^{133}Ba not actually incorporated into the ferrihydrite matrix, the colloidal sol is extensively rinsed by dialysis. The Fe/ ^{133}Ba ratio in the final rinsed phase is about 10 5 /1. A fresh batch of ferrihydrite was synthesized for each experiment.

Photochemical experiments with irradiation system—The irradiation system consisted of a 1,000W Hg/Xe lamp equipped with an infrared filter and a pyrex ultraviolet filter. The lamp produced a broad spectrum (300–800 nm) beam of light, with an intensity about 10 times that of natural sunlight.

Colloidal ferrihydrite colabeled with ^{133}Ba and ^{59}Fe was synthesized as described above and added to various water samples at a concentration of approximately 2 μM Fe. After a period of equilibration, 30-ml aliquots were loaded into a quartz spectrophotometric cell (10 cm length) for irradiation. Samples were irradiated in front of the light source for 1 h. A small ($\sim 5^\circ\text{C}$) increase in sample temperature was observed over this period.

For determination of dissolved ^{133}Ba and ^{59}Fe , irradiated and nonirradiated samples were syringe-filtered through a 47 mm diameter, 0.05 μm pore-size Nuclepore polycarbonate filter. Unfiltered aliquots were also taken for determination of total ^{133}Ba and ^{59}Fe . ^{133}Ba and ^{59}Fe activity in filtrates and totals was determined on a Canberra low-energy germanium detector.

Replicate photochemical experiments were carried out in

a suite of unfiltered natural waters. (See Table 1 for information on salinity, pH, and light attenuation of each water type). ^{133}Ba -ferrihydrite was added to each water sample and allowed to equilibrate for 1 h prior to irradiation. Following irradiation, filtrate and total samples were taken for irradiated samples and dark controls. (Due to the possibility of light attenuation, the Salt Pond and "Estuary" samples were mixed and turned around every 15 min. during irradiation.)

A second series of photochemical experiments was performed with the VSW, SSW, and WB water types. ^{133}Ba -ferrihydrite was added to each water type and allowed to incubate overnight prior to photochemical irradiation. Half of the water samples were incubated overnight at room temperature, and half were incubated at 4°C. Irradiations were performed the next day and filtrate and total samples were taken for irradiated samples and dark controls as described above. There were no replicate irradiations in this experiment.

Photochemical experiment in natural sunlight—A photochemical experiment was conducted in natural sunlight in Vineyard Sound seawater on 8 July 1997. Colloidal ferrihydrite colabeled with ^{133}Ba and ^{59}Fe was added to both 0.2 μm -filtered and unfiltered VSW at a concentration of about 3 μM Fe, and equilibrated overnight at 4°C. At 1000 h, both filtered and unfiltered VSW/ferrihydrite solutions were placed in quartz flasks and irradiated under natural sunlight until 1600 h. During irradiation, flasks were submerged in a circulating water bath which maintained the water temperature at 19°C. Foil-wrapped flasks served as dark controls. Irradiated flasks and dark controls were sampled at intervals for dissolved and total ^{133}Ba and ^{59}Fe . There were no replicates in this experiment.

Grazing experiment in a model system—Reasoning that the photochemical reduction of iron oxides could potentially be greatly accelerated within the acidic, reducing microenvironment of the grazer food vacuole, a grazing experiment was conducted to examine the possibility of synergistic effects of grazing and photochemistry on the dissolution of colloidal ferrihydrite.

Table 2. Size* fractions and treatments set up for grazing experiment with natural consortium.

Radiolabeled† incubations			
Series 1 Bacteria plus ferrihydrite	Series 2 Ferrihydrite only	Series 3 ¹³³ Ba only	Nonlabeled‡ incubations
<200 μm	<200 μm	<200 μm	<200 μm
<20 μm	<20 μm	<20 μm	<20 μm
<200 μm + MI§	<200 μm + MI		<200 μm + MI
<1 μm	<1 μm		
<0.2 μm	<0.2 μm		

* All types of incubations shown were set up in replicate.

† Series 1 and 2 radiolabeled incubations contained ¹³³Ba/⁵⁹Fe colabeled colloidal ferrihydrite added at 1–2 μM Fe concentration. Series 1 contained ¹³³Ba/⁵⁹Fe ferrihydrite added in association with heat-killed bacteria; Series 2 contained ¹³³Ba/⁵⁹Fe ferrihydrite only. Series 3 contained only dissolved ¹³³Ba.

‡ Nonlabeled incubations contained only DTAF-stained bacteria to follow grazing rates (see text).

§ MI = metabolic inhibitor (colchicine and cyclohexamide, see text).

A grazing experiment was set up in quartz flasks, irradiated by cool-white fluorescent light at an intensity of approximately 300 μEinstein m⁻² s⁻¹. The grazer used in this experiment was the heterotrophic flagellate *Cafeteria* sp. (2–4 μm in size, clone Cflag). The bacteria used as prey were heterotrophic marine bacteria, *Halomonas halodurans*. Both organisms were obtained from the culture collection of D. Caron at WHOI. Bacteria were heat-killed by incubation for 2 h at 60°C and rinsed by centrifugation three times (in VSW) before resuspension in model systems. Protozoan cultures were maintained on heat-killed bacteria for at least three transfers prior to being inoculated into experimental cultures. The following radiolabeled model systems were set up (each in replicate) for this experiment, each with 2 μM ¹³³Ba/⁵⁹Fe ferrihydrite added and with VSW as the base medium: *Cafeteria* with heat-killed bacteria, irradiated, 300-ml quartz flask; *Cafeteria* with heat-killed bacteria, foil-wrapped, 300-ml quartz flask; and heat-killed bacteria, irradiated, 100-ml quartz flask.

The following nonlabeled model systems were set up (in replicate) to sample for bacteria and protozoan cell counts: *Cafeteria* with heat-killed bacteria, irradiated, 100-ml quartz flask; and *Cafeteria* with heat-killed bacteria, foil-wrapped, 100-ml glass flask.

At t_0 , the bacteria concentration in all flasks was $\sim 1.2 \times 10^7$ cells ml⁻¹. *Cafeteria* was inoculated (from an exponential phase culture) to give an initial concentration of $\sim 4.4 \times 10^3$ cells ml⁻¹. Flasks (including those wrapped in foil) were all incubated in front of the fluorescent lights at room temperature, without agitation except prior to sampling. Irradiated and foil-wrapped radiolabeled grazing cultures were sampled for dissolved (0.05 μm syringe-filtered) and total ¹³³Ba every 12 h. The radiolabeled bacteria-only control was sampled every 24 h. Nonlabeled cultures were sampled every 12 h for cell counts. Samples for cell counts were preserved in 1% glutaraldehyde until slides were made for epifluorescence counting using acridine orange staining.

Grazing experiment with natural consortium—Vineyard Sound seawater for this grazing experiment was collected at 0900 h on 18 September 1997 on an incoming tide off the WHOI dock. Water temperature at the time of collection was 21°C. Immediately after collection, water was transported

back to the laboratory for size fractionation and experimental set-up. Water was gently filtered by gravity through the following size cutoffs: 200, 20, 1, and 0.2 μm. All filters, filter holders, filter cartridges, tubing, and connectors were acid cleaned, as were the incubation bottles.

Table 2 details the radiolabeled and nonlabeled size fractions and incubation treatments that were set up for this experiment, each in duplicate. The nonlabeled incubations and the Series 1 and 2 radiolabeled incubations were set up in 1-L polycarbonate bottles filled to 500 ml. The Series 3 radiolabeled incubations were set up in 250 ml polycarbonate bottles filled to 125 ml. The metabolic inhibitors, colchicine and cyclohexamide (concentrations 100 and 200 mg L⁻¹, respectively) have been shown to inhibit grazing by eukaryotic organisms without adverse effects on prokaryotes (Sherr et al. 1986; Caron et al. 1991). Metabolic inhibitors were added 1 h prior to adding Fe colloids or bacteria to incubations.

Heat-killed bacteria stained with 5-(4,6-dichlorotriazin-2-yl)aminofluorescein (DTAF) (Sigma) were added to nonlabeled incubations (see Table 2) in order to follow grazing rates. DTAF-stained bacteria (*H. halodurans*) were prepared according to the protocol of Sherr et al. (1987). Bacteria were added to both the nonlabeled incubations and the Series 1 radiolabeled incubations (see Table 2) at a concentration of $\sim 3.8 \times 10^6$ cells ml⁻¹.

Colloidal ferrihydrite colabeled with ¹³³Ba and ⁵⁹Fe was added to the Series 1 and 2 radiolabeled incubations at concentrations of 1–2 μM iron. In the Series 2 radiolabeled incubations, only colloidal ferrihydrite was added. In the Series 1 radiolabeled incubations, the ¹³³Ba/⁵⁹Fe-labeled ferrihydrite was added in association with bacteria cells so that ferrihydrite dissolution could be correlated with the rate of bacteria (and associated ferrihydrite) consumption. To ensure association of the ferrihydrite with bacterial cells, bacteria and ferrihydrite colloids were combined in VSW for several hours before the start of the experimental incubations, at a concentration of 10⁷ cells ml⁻¹ bacteria and 10⁻⁵ M Fe as colloidal ferrihydrite. Association of Fe colloids with bacteria cells was evidenced by the visible formation of orange flocs. Mixed aliquots of the bacteria/colloidal iron suspension were briefly ultrasonicated to disperse aggregates just

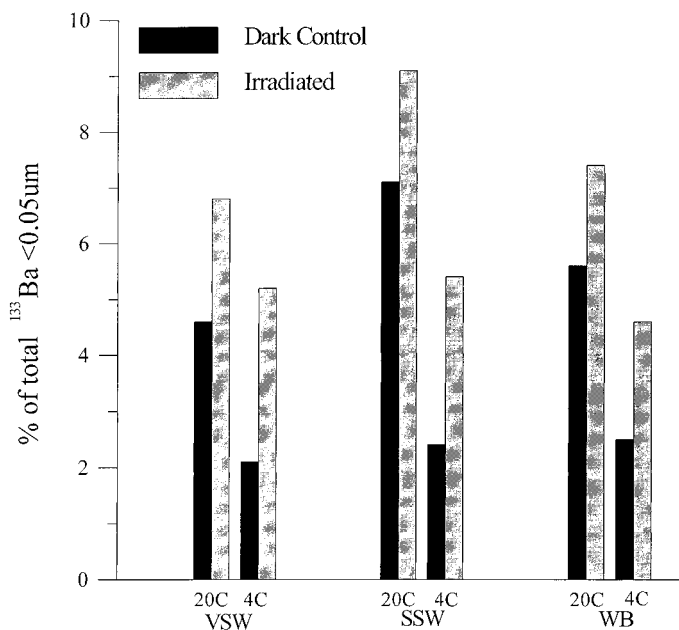


Fig. 1. Photochemical and thermal effects—percentage of dissolved ^{133}Ba produced upon irradiation of ferrihydrite incubated overnight at 4°C vs. 20°C in Vineyard Sound seawater (VSW), Sargasso seawater (SSW) and Waquoit Bay water (WB). Irradiation time is 1 h. The y-axis shows percentage of dissolved ^{133}Ba (as defined by $0.05\ \mu\text{m}$ filtration) relative to total ^{133}Ba activity in sample.

prior to adding at 1/10 dilution (10^6 cells ml^{-1} , 10^{-6} M Fe) to Vineyard Sound seawater in incubation bottles.

The Series 3 radiolabeled incubations, $<200\ \mu\text{m}$ and $<20\ \mu\text{m}$ size fractions spiked with dissolved ^{133}Ba , were set up as controls for the adsorption of dissolved ^{133}Ba by particles and bottle walls.

All bottles were incubated for 5 days at a temperature between 18°C and 20°C , on a 12-h light/dark cycle. Series 1 and 2 radiolabeled bottles were sampled every 24 h for dissolved ($0.05\ \mu\text{m}$ Nuclepore filter syringe filtration) and total ^{133}Ba . The Series 3 ^{133}Ba -spiked bottles were sampled at t_0 , t_{24} , t_{72} , and t_{120} for total and $0.2\ \mu\text{m}$ filterable (Millipore, 25 mm diameter) ^{133}Ba . Filtrate and total samples were prepared and counted for radioactivity as previously described.

Nonlabeled incubations were sampled every 24-h and preserved in 1% glutaraldehyde for cell counts. In addition to slides for DTAf-bacteria, slides stained with 4',6-diamidino-2-phenylindole were also prepared in order to examine the natural consortium of the field sample and various size fractions (Porter and Feig 1980). Slides were examined by epifluorescence microscopy.

Results and discussion

Photochemical experiments with irradiation system—The results of the 1 h irradiations after brief equilibration in VSW, SSW, WB, "Estuary," and Salt Pond are shown in Table 1. All of these waters exhibited some degree of photoactivity, as indicated by higher dissolved ^{133}Ba in the irradiated samples. (No increase in dissolved ^{59}Fe was de-

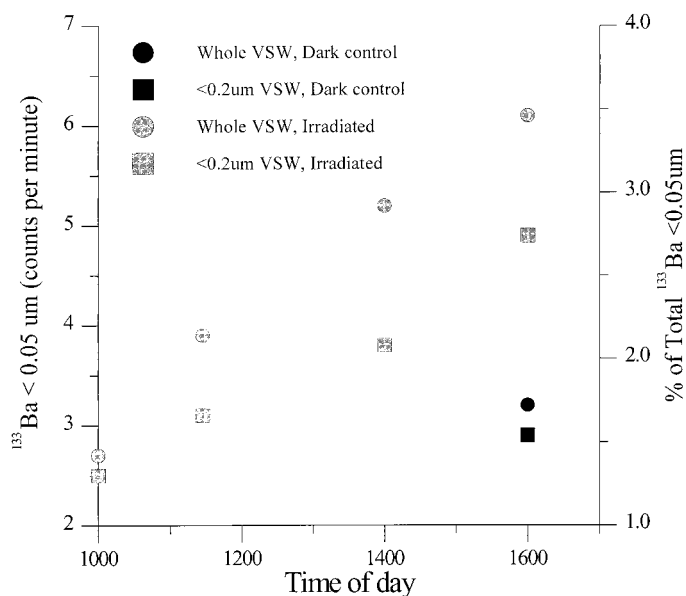


Fig. 2. Natural sunlight experiment—production of dissolved (i.e., $<0.05\ \mu\text{m}$) ^{133}Ba in filtered and unfiltered Vineyard Sound seawater (VSW) upon irradiation of a ferrihydrite suspension in natural sunlight. The y-axes show dissolved ^{133}Ba both in terms of raw counts per minute (left axis) and as a percentage of the total ^{133}Ba activity in the sample (right axis).

ected.) For most of these waters, the rate constant of dissolved ^{133}Ba release by photodissolution over the 1 h irradiation period (calculated as the difference between irradiated samples and dark controls, assuming linear kinetics) was between $0.019 \pm 0.004\ \text{h}^{-1}$ and $0.029 \pm 0.001\ \text{h}^{-1}$. The exception was the Salt Pond sample, which had a rate constant of $0.046 \pm 0.03\ \text{h}^{-1}$, possibly due to the higher concentration of dissolved chromophores as well as the lower pH in this water type relative to the others.

Figure 1 shows the data for ferrihydrite equilibrated overnight in VSW, SSW, and WB at room temperature and at 4°C . In terms of release of dissolved ^{133}Ba over 1 h irradiation, the overnight equilibration time did not make a significant difference relative to the data in Table 1. Rates of photochemically-mediated ^{133}Ba release still varied between about $0.02\ \text{h}^{-1}$ and $0.03\ \text{h}^{-1}$ for all these samples, as in the shorter equilibration experiment. This data indicates that the timescale for adsorption of organic chromophores onto the iron oxide surfaces is not limiting to the photoreduction observed after equilibrations of an hour or more. Adsorption of organics by the colloidal ferrihydrite must therefore be relatively rapid, as hypothesized by Wells and Mayer (1991).

The most striking difference in this experiment was in the dark controls, between those equilibrated overnight at 4°C vs. those equilibrated at room temperature (Fig. 1). Percentage dissolved ^{133}Ba was at least twice as high in the room temperature dark controls, possibly due to higher rates of thermal dissolution at room temperature relative to 4°C . Maturation reactions of the ferrihydrite might also explain this data. Faster maturation reactions at higher temperatures could cause some rearrangement of the iron oxide matrix, resulting in the release of ^{133}Ba to the dissolved phase. In

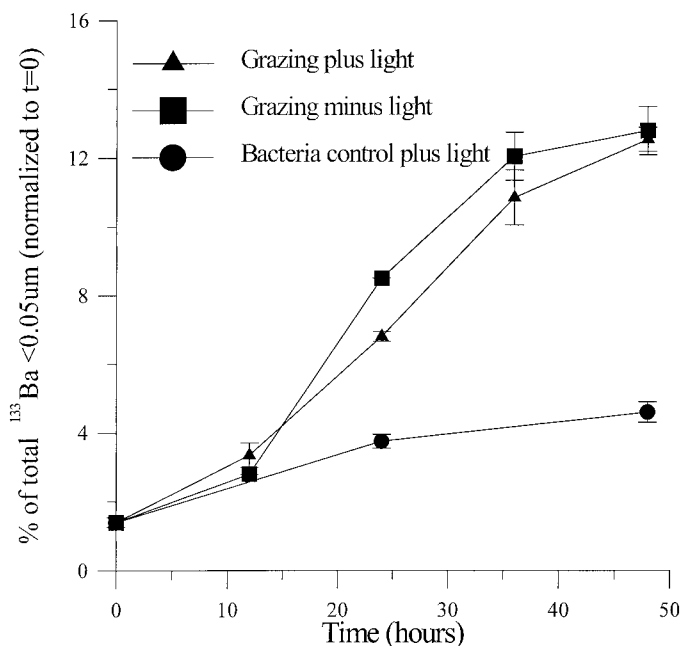


Fig. 3. Interactive effects of grazing and light—production of dissolved ^{133}Ba in irradiated and nonirradiated *Cafeteria* grazing cultures, relative to irradiated bacteria control. The y-axis shows the increase in percentage of dissolved ^{133}Ba relative to the total ^{133}Ba in the system at t_0 .

addition to thermal dissolution and/or maturation, the dissolved ^{133}Ba in the dark controls may also reflect ion exchange and sorption/desorption reactions taking place at the ferrihydrite surface upon addition to seawater from the Milli-Q water dialysis matrix. The rate of these reactions may also be positively correlated with temperature.

Photochemical experiment in natural sunlight—Both filtered and unfiltered irradiated VSW flasks demonstrated an increase in dissolved ^{133}Ba relative to the dark controls (Fig. 2). No dissolved ^{59}Fe was observed in any filtrates. The initial rate constant for production of dissolved ^{133}Ba from 1000 h to 1130 h was 0.005 h^{-1} in unfiltered VSW, and 0.003 h^{-1} in filtered VSW. These rate constants are about an order of magnitude lower than what was observed for photolysis in VSW using the irradiation system. This is consistent with the $\sim 10\times$ lower light intensity in natural sunlight relative to the 1,000W Hg/Xe lamp. Waite and Morel (1984) observed a linear relationship between light intensity and photoreduction rate.

The rate of production of dissolved ^{133}Ba was higher in the unfiltered VSW than in the filtered VSW. This is consistent with the work of Johnson et al. (1994), who observed increased rates of colloidal iron photolysis in unfiltered vs. filtered equatorial Pacific water. The higher rate of reaction in unfiltered water may be due to the interaction of colloidal ferrihydrite with particle surfaces. It is possible that the presence of additional adsorptive surfaces for photoproduct dissolved Fe species allows a greater chance for ^{133}Ba to escape from the Fe oxide lattice. Particles might also increase re-

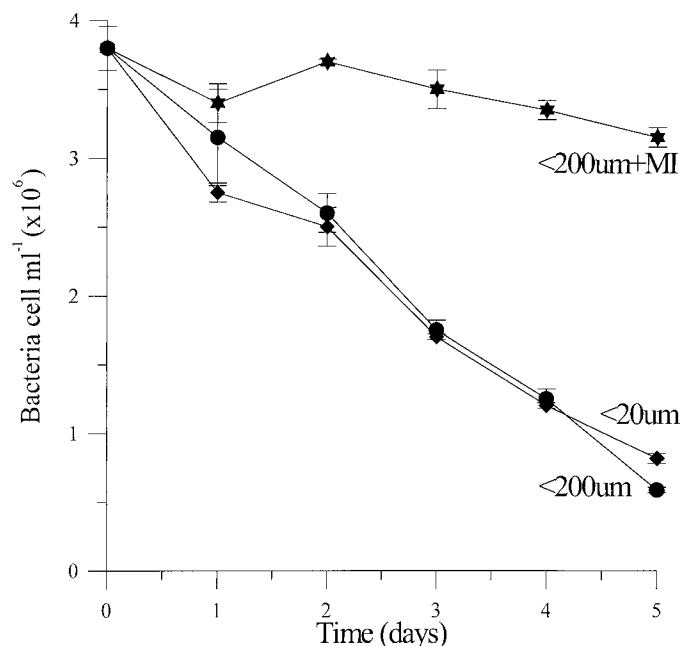


Fig. 4. Grazing experiment with natural consortium—decrease in concentration of DTAF-stained bacteria over time in nonlabeled incubations. The y-axis shows concentration of DTAF-stained bacteria in cells ml^{-1} .

action rates by providing a source of reactive chromophores close to iron oxide surfaces.

The colloidal Fe photolysis rate in unfiltered VSW derived here (0.005 h^{-1}) is a factor of 3–4 less than the oxine lability photoreduction rate measured by Wells and Mayer (1991) for ferrihydrite incubated in surface seawater under natural sunlight at 13.5°C (Wells and Mayer 1991; rate constant estimated from Fig. 5 = $0.016\text{--}0.018\text{ h}^{-1}$). Considering the differences between the ^{133}Ba method and the oxine lability method, the two rates agree fairly well. There are a number of reasons, aside from intrinsic differences between the two techniques, why our observed rate constant could be lower. Our colloids are almost certainly more refractory (and therefore slower to react) than those used by Wells and Mayer (1991), given that they are extensively dialyzed prior to use in experiments. Additional factors that may account for the difference include time of day and incubation temperature.

Grazing experiment in model system—Results are shown in Fig. 3 for production of dissolved ^{133}Ba in the irradiated and nonirradiated grazing cultures, and in the irradiated bacteria control. Both of the grazing cultures demonstrated elevated levels of dissolved ^{133}Ba relative to the bacteria control (by about a factor of 3), indicating grazer-mediated dissolution of colloidal iron oxide. There was little difference between the irradiated and nonirradiated grazing cultures with regard to production of dissolved ^{133}Ba . Cell counting data from the nonlabeled cultures indicate that protozoans in the irradiated and nonirradiated grazing cultures consumed bacteria at similar rates (data not shown), and by t_{48} bacteria concentrations had been reduced to similar levels in both ($1.14 \pm 0.16 \times 10^6$ cells ml^{-1} in irradiated cultures; $1.0 \pm 0.5 \times 10^6$ cells ml^{-1} in nonirradiated cultures). *Caf-*

eteria cell counts indicate that there may have been some light inhibition of *Cafeteria* growth in the irradiated cultures—protozoan cell yields at t_{48} were a factor of 2.5 times lower in the irradiated vs. the nonirradiated cultures ($4.4 \pm 0.8 \times 10^4$ cells ml^{-1} vs. $1.1 \pm 0.2 \times 10^5$ cells ml^{-1}). This may account for the small lag in production of dissolved ^{133}Ba in Fig. 3 in the irradiated vs the nonirradiated grazing cultures.

In summary, there is little evidence in these data to indicate that light enhanced the dissolution of colloidal ferrihydrite in the irradiated grazing cultures. The extent of colloidal ferrihydrite dissolution appeared to be determined solely by grazer activity. Different results might be obtained with higher light levels, although more intense light could potentially inhibit the grazers. As the results in the irradiated bacteria control demonstrate, a light intensity of $300 \mu\text{-Einstein m}^{-2} \text{s}^{-1}$ was insufficient by itself to enhance dissolution of the colloidal ferrihydrite.

Grazing experiment with natural consortium—Figure 4 shows the decrease in concentration of DTAF-stained bacteria in the nonlabeled incubations in the grazing experiment with a natural consortium. The metabolically inhibited incubations had a greatly reduced rate of bacteria removal, and the noninhibited $<200 \mu\text{m}$ and $<20 \mu\text{m}$ incubations (i.e., those containing active grazer populations) demonstrated a rate of decrease in concentration of the DTAF-stained bacteria of about 18% per day.

Over the 5-day time course of this experiment, significant decreases in the total activity of ^{133}Ba and ^{59}Fe were observed in the Series 1 and 2 incubation bottles that contained an active grazer population. The observed loss of ^{133}Ba and ^{59}Fe activity is interpreted to be due to the adhesion of $^{133}\text{Ba}/^{59}\text{Fe}$ -colabeled colloidal ferrihydrite to bottle walls (i.e., wall loss). Series 3 radiolabeled $<200 \mu\text{m}$ and $<20 \mu\text{m}$ incubations spiked with dissolved ^{133}Ba demonstrated no wall loss of dissolved ^{133}Ba by day 5 of the incubation relative to the dissolved ^{133}Ba activity added to each bottle at t_0 . Uptake of ^{133}Ba onto particles $>0.2 \mu\text{m}$ in those incubations by day 5 was also minor, $1.45 \pm 0.6 \%$ in the $<200 \mu\text{m}$ incubations, and $0.07 \pm 0.02 \%$ in the $<20 \mu\text{m}$ incubations. Thus dissolved ^{133}Ba was shown to remain stable in the solution phase over a 5 day incubation. Loss of ^{133}Ba activity apparently occurred in the grazing incubations as a consequence of ^{133}Ba -labeled ferrihydrite adsorption to bottle walls.

The effect of wall loss on the interpretation of dissolved ^{133}Ba data must be considered. In order to determine a specific rate of dissolution, dissolved ^{133}Ba must be normalized to the total ^{133}Ba pool either at $t = 0$ (i.e., the start of the experiment) or at time t (any sample point thereafter). Percentage of dissolved ^{133}Ba produced in Series 1 and Series 2 incubations is shown in Fig. 5 normalized to ^{133}Ba activity at t_0 . In Fig. 6, the same data are shown normalized to the total ^{133}Ba activity in each incubation treatment at each time point (time t). Normalizing to time t assumes that only the reservoir of colloidal ferrihydrite remaining in suspension can contribute to the accumulation of dissolved ^{133}Ba . If ferrihydrite adsorbed to the bottle walls is also undergoing dissolution, then a dissolution rate normalized to time t (Fig. 6) will significantly overestimate the rate in the bulk solution. However, if the grazer-mediated dissolution rate of colloidal ferrihydrite adsorbed to the wall is considerably slow-

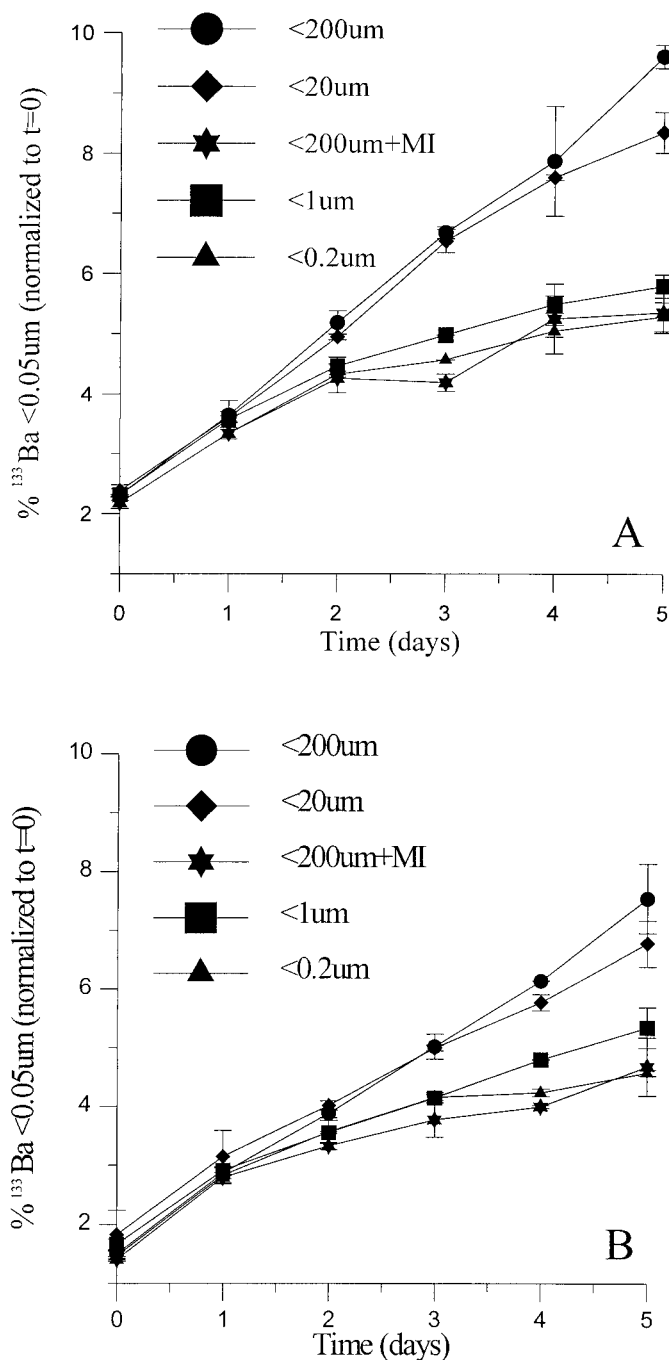


Fig. 5. Grazing experiment with natural consortium—percentage of dissolved ^{133}Ba production in different incubation treatments over time, normalized to t_0 . (A) Series 1, ^{133}Ba -ferrihydrite added with bacteria; (B) Series 2, ^{133}Ba -ferrihydrite added alone.

er, then normalizing to t_0 (Fig. 5) will significantly underestimate the dissolution rate for suspended ferrihydrite.

The data in Fig. 5, percentage of dissolved ^{133}Ba normalized to t_0 , can be taken as a *minimum estimate* of the effects of the natural grazing consortium on colloidal ferrihydrite reactivity. The rate of dissolved ^{133}Ba increase for all treatments is the same from t_0 to t_{24} . This initial rate is largely a

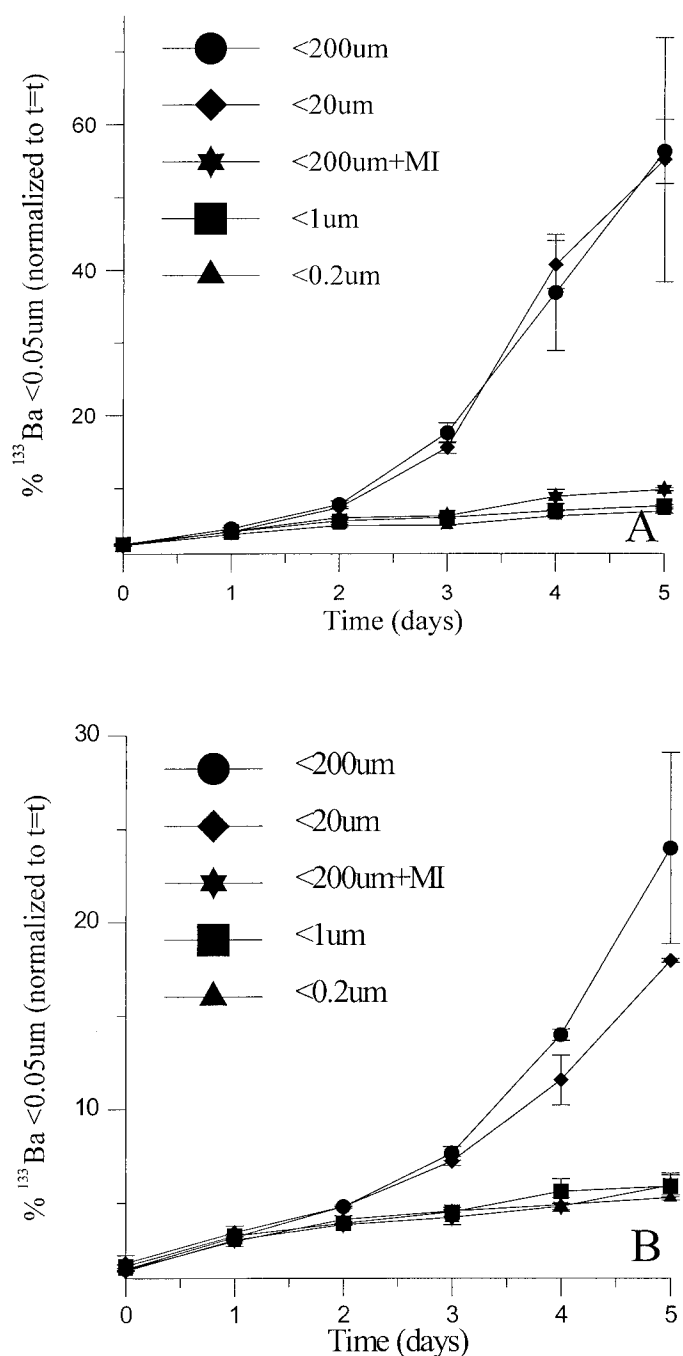


Fig. 6. Grazing experiment with natural consortium—percentage of dissolved ^{133}Ba production in different incubation treatments over time, normalized to time t . (A) Series 1, ^{133}Ba -ferrihydrite added with bacteria; (B) Series 2, ^{133}Ba -ferrihydrite added alone.

function of the release of ^{133}Ba from the ^{133}Ba -impregnated colloids upon addition to seawater. This release is due to either a small excess of ^{133}Ba that was not rinsed away by dialysis, ion exchange with alkaline earths in seawater, and/or conformational changes in the ferrihydrite that occur due to the change from a Milli-Q water matrix to seawater. In the nongrazing controls, particularly in the metabolically in-

hibited and $<0.2\mu\text{m}$ filtered controls, this rate flattens out perceptibly after about 48 h. In the grazing incubations, the relatively fast initial rate of increase in dissolved ^{133}Ba is maintained over the entire 5 day period, presumably due to the dissolution of colloidal ferrihydrite by the grazers.

The rate of increase in dissolved ^{133}Ba in Fig. 5A, for the noninhibited $<200\mu\text{m}$ incubations in radiolabeled Series 1, is about 1.5% per day over the entire time course. In the nongrazing controls, the rate of increase in dissolved ^{133}Ba after 48 h (the period of equilibration and relatively faster ^{133}Ba release) is about 0.3% per day. Subtracting this from the rate of increase in the grazing cultures, we obtain a rate of increase in dissolved ^{133}Ba due to grazing of about 1.2% per day. Normalizing to the consumption of DTAF-labeled bacteria (and associated ferrihydrite colloids) in those cultures (Fig. 4; -17.6% per day), this indicates a colloidal ferrihydrite dissolution efficiency of the indigenous grazer population of about 7%. This figure is in fairly good agreement with the estimated dissolution efficiency for a natural grazing consortium derived previously (8.25%; Barbeau and Moffett 1998).

The results for the Series 2 incubations were fairly similar to Series 1. The rate of increase in dissolved ^{133}Ba in the noninhibited $<200\mu\text{m}$ incubation in Fig. 5B, corrected in the same way as above for dissolution after 48 h in the controls, is about 1% per day. The apparent difference between the grazing cultures and controls in Series 2 (Fig. 5B) is lessened due to the somewhat elevated rate of dissolution in the $>1\mu\text{m}$ control in Series 2. The observed dissolution in the $>1\mu\text{m}$ control could be due to prokaryote activity, or due to the presence of small flagellates not removed by $1\mu\text{m}$ filtration. One possible factor contributing to the difference between Series 1 and Series 2 is that the enrichment of Series 1 systems with 3.8×10^6 cells ml^{-1} bacteria likely caused an increase in the grazer population by day 5. This could account for the somewhat elevated rate of colloidal ferrihydrite dissolution in Series 1 relative to Series 2. Another contributing factor could be lower ingestion rates (i.e., turnover) of the colloidal Fe in Series 2. Since the ferrihydrite was added by itself without being preassociated with bacterial cells as in Series 1, it could have been scavenged by a variety of indigenous particles present in the seawater, many of which may not have been amenable to grazing.

Turnover is a key parameter in the calculation of protozoan-mediated iron oxide dissolution rates. In a previous work (Barbeau and Moffett 1998) we derived a range of rate constants for refractory iron dissolution by grazers in natural waters, from a minimum of 1.7% per day to a maximum of 5.8% per day, depending on turnover rates (i.e., grazing rates, published ranges 20–70% per day; e.g., Valiela 1995). In this study, minimal estimates of the rate of colloidal iron oxide dissolution by a natural grazing consortium, based on the data in Fig. 5, are about 1% per day. A maximal rate estimate of 4–6% per day is obtained from the data in Fig. 6, where dissolved ^{133}Ba is normalized to total ^{133}Ba at time t . This is analogous to the use of a higher turnover rate in our previously published estimate, since normalizing to the ^{133}Ba total at time t is equivalent to reducing the grazer-available pool of ^{133}Ba (and thereby increasing the turnover rate of ^{133}Ba in a system at a constant grazing rate). Thus, in this field study we have derived a range of 1–6% per day

for the protozoan-mediated dissolution of refractory iron solids in natural waters. This range is comparable to that derived from our previous laboratory studies, 1.7–5.8 % per day (Barbeau and Moffett 1998). Given that protozoan-mediated dissolution of refractory iron is, of necessity, related to the rate of turnover of bacterial biomass (and associated refractory iron) by protozoan grazers, it is not possible to narrow our estimate range any further.

Another factor that has not been considered in this discussion is the possibility of uptake of ^{133}Ba across the vacuolar membrane of grazing organisms, perhaps as an analog of Ca. While Ba uptake is certainly a possibility, we expect its influence on our results to be minor relative to the influence of overall grazing turnover rate.

Rate comparison of photochemical and grazer-mediated ferrihydrite dissolution—In this work, the rate of colloidal iron oxide dissolution by photolysis was measured in natural sunlight in Vineyard Sound seawater, at 1 μM concentration Fe. In unfiltered seawater, the maximal initial photolysis rate was determined to be about 12% per day. The rate of protozoan-mediated dissolution of colloidal iron oxides has been measured previously in several laboratory culture experiments (Barbeau and Moffett 1998), and in this work in field incubation experiments with natural consortia. As described above, these measurements converge on a range of 1–6% per day for protozoan-mediated dissolution of colloidal iron oxides in natural waters, depending on grazing turnover rates.

The rate comparison above, while it is the first of its kind, is specific to the ^{133}Ba -impregnated ferrihydrite used in this study. It is difficult to more generally compare the rate of protozoan-mediated dissolution with the rate of photoreductive dissolution of iron oxides. Few measurements have been made of iron oxide photoreduction rates in seawater at pH 8, and there are significant differences amongst the rate constants obtained by various investigators (e.g., Waite and Morel 1984; Johnson et al. 1994; Wells and Mayer 1991, this study) due to differences in the concentration of iron oxide, the degree of reactivity of the iron oxide phase, experimental conditions, and detection methods. Thus there is not a universally-accepted value for the rate of iron oxide photolysis in seawater to which protozoan-mediated dissolution can be compared.

Another difficulty that arises in this comparison is that the few photoreduction rates that have been measured represent near-surface maximum rates, which must be extrapolated and integrated to obtain average values with depth and over time. Johnson et al. (1994) attempted to do this with a model of iron cycling in seawater at the equatorial Pacific. Their maximum photoreduction rate in the upper 10 m, 25 $\text{pmol Fe L}^{-1} \text{h}^{-1}$, dropped to an average rate of only 2 $\text{pmol Fe L}^{-1} \text{h}^{-1}$ when integrated over a 24 h cycle at light intensities from the surface to the 0.1% light level (75 m). This model was for an oligotrophic open ocean region. As shown by Wells et al. (1991), the attenuation of photochemically active light occurs at much shallower depths in coastal areas (5–10 m) vs. open ocean waters (100 m). The depth of light penetration is also dependent on the assumed wavelength dependence of iron oxide photoreduction, which is currently not very well-constrained.

Mechanism of dissolution and extrapolation to other iron phases—Consideration of the possible causative factors responsible for grazer-mediated ferrihydrite dissolution enables us to make a reasonable extrapolation to other forms of iron likely to be important in seawater. The dissolution of iron oxides is known to be accelerated by: (a) reducing agents, (b) strong iron chelators, and (c) decreased pH (Deng and Stumm 1994; Moffett in press). It is plausible that at least one, and possibly all three of these factors exist within protozoan food vacuoles and favor ferrihydrite dissolution. Given that assumption, it is likely that other solid phases of iron would also undergo dissolution under vacuole conditions.

For example, solid forms of iron comprised of Fe-organic complexes, a significant reservoir of iron in oceanic regimes (Rue and Bruland 1995; Wu and Luther 1995), would undergo accelerated dissolution under all three conditions noted above. The strongest iron complexes are with ligands containing phenolic, hydroxamate and amine groups that have high pKa's and are readily demetallated at low pH. Moreover, ligand substitution reactions of strong iron chelators like siderophores occur rapidly in the presence of strong competing ligands and reductants (Crumbliss, 1991). Barbeau (1998) showed that iron organically associated with bacteria cells is readily converted into dissolved phases during protozoan grazing, consistent with this prediction. Thus, we feel that our results with ferrihydrite as a model phase have important implications for uncharacterized solid phases of iron and organic matter. In contrast, detrital particulate iron, defined operationally as that fraction which is only labile analytically when treated with concentrated acids (Landing and Lewis 1991), is unlikely to be reactive in the grazing process.

Extrapolation of our ferrihydrite photolysis rate data to Fe-organic solids is more problematic, because Fe-organic complexes exhibit a range of photolysis rates depending on their chemical structure and absorption spectra of ligand-to-metal charge transfer bands. Fe(III) carboxylate ligands like citrate and oxalate, for example, are highly photoreactive (Faust and Zepp 1993), while Fe(III) hydroxamate ligands like the siderophore deferriferrioxamine B have been shown to be non-photoreactive (Gao and Zepp 1998). Thus while it seems likely, based on vacuole chemistry, that grazing influences the redox cycling of a wide variety of iron solid phases in seawater, it is more difficult to compare the relative importance of grazing and photochemistry across a similar spectrum of iron solids due to the likelihood of substantial variation in photochemical reactivity.

Conclusions—A novel inert tracer technique was used to study photochemical and grazer-mediated transformations of a model iron oxide phase, colloidal ferrihydrite. Results with a high-intensity artificial light source indicated little qualitative difference in the photochemical reactivity of a suite of natural waters, in terms of ferrihydrite reactivity as assayed by our method. In a study of the interactive effects of protozoan grazing and light, white light at a flux of 300 $\mu\text{Einsteins m}^{-2} \text{s}^{-1}$ was shown to have no significant effect on colloidal ferrihydrite dissolution relative to grazing. Light also did not appear to enhance the extent of dissolution occurring within grazer food vacuoles.

In a new rate comparison on the same iron oxide phase,

at the same concentration in Vineyard Sound seawater, as determined by the same ^{133}Ba measurement technique, it was demonstrated that protozoan-mediated dissolution of colloidal iron oxides in natural waters proceeds at a rate which is one-tenth to one-half of the maximal, noon-time near-surface rate of photochemically-mediated dissolution of iron oxides. The relative magnitude of these two rates is similar to that obtained in previous, less direct, estimates (Barbeau et al. 1996). It is argued on the basis of these measurements that, on a time- and depth-integrated basis, protozoan grazers are likely to be more important than photochemistry as an influence on the redox cycling of particulate and colloidal iron in oxygenated seawater.

References

- BARBEAU, K. 1998. Influence of protozoan grazing on the marine geochemistry of particle reactive trace metals. Ph.D. Thesis. MIT/WHOI Joint Program in Oceanography.
- , AND J. W. MOFFETT. 1998. Dissolution of iron oxides by phagotrophic protists: Using a novel method to quantify reaction rates. *Env. Sci. Technol.* **32**: 2969–2975.
- , ———, D. CARON, P. L. CROOT, AND D. ERDNER. 1996. Role of protozoan grazing in relieving iron limitation of phytoplankton. *Nature* **380**: 61–64.
- CARON, D., E. L. LIM, G. MICELI, J. B. WATERBURY, AND F. W. VALOIS. 1991. Grazing and utilization of chroococcoid cyanobacteria and heterotrophic bacteria by protozoa in laboratory cultures and a coastal plankton community. *Mar. Ecol. Prog. Ser.* **76**: 205–217.
- COALE, K. H., AND OTHERS. 1996. A massive phytoplankton bloom induced by an ecosystem-scale iron fertilization experiment in the equatorial Pacific Ocean. *Nature* **383**: 495–501.
- CRUMBLISS, A. L. 1991. Aqueous solution equilibrium and kinetic studies of iron siderophore and model siderophore complexes, p. 177–233. *In* G. Winkelmann [ed.], *CRC handbook of microbial iron chelates*. CRC Press.
- DE BAAR, H.J.W., A.G.J. BUMA, R. F. NOLTING, G. C. CADEE, G. JACQUES, AND P. J. TREGUER. 1990. On iron limitation of the Southern Ocean: Experimental observations in the Wedell and Scotia Seas. *Mar. Ecol. Prog. Ser.* **65**: 105–122.
- DENG, Y., AND W. STUMM. 1994. Reactivity of aquatic iron(III) oxyhydroxides—implications for redox cycling of iron in natural waters. *Appl. Geochem.* **9**: 23–36.
- FAUST, B. C., AND R. G. ZEPP. 1993. Photochemistry of aqueous iron(III)-polycarboxylate complexes: Roles in the chemistry of atmospheric and surface waters. *Environ. Sci. Technol.* **27**: 2517–2522.
- FISHER, N. S., R.R.L. GUILLARD, AND D. C. BANKSTON. 1991. The accumulation of barium by marine phytoplankton grown in culture. *J. Mar. Res.* **49**: 339–354.
- GAO, H., AND R. G. ZEPP. 1998. Factors influencing photoreactions of dissolved organic matter in a coastal river of the Southeastern United States. *Environ. Sci. Technol.* **32**: 2940–2946.
- HUTCHINS, D. A., AND K. W. BRULAND. 1998. Iron-limited diatom growth and Si:N uptake ratios in a coastal upwelling regime. *Nature* **393**: 561–564.
- JOHNSON, K. S., K. H. COALE, V. A. ELROD, AND N. W. TINDALE. 1994. Iron photochemistry in the equatorial Pacific. *Mar. Chem.* **46**: 319–334.
- LANDING, W. M., AND B. L. LEWIS. 1991. Collection, processing, and analysis of marine particulate and colloidal material for transition metals, p. 263–272. *In* D. C. Hurd and D. W. Spencer [eds.], *Marine particles: Analysis and characterization*. AGU Geophysical Monograph Series.
- LANDRY, M. R., AND OTHERS. 1997. Iron and grazing constraints on primary production in the central equatorial Pacific: An EqPac synthesis. *Limnol. Oceanogr.* **42**: 405–418.
- LI, Y.-H., L. BURKHARDT, M. BUCHHOLTZ, P. O'HARA, AND P. H. SANTSCHI. 1984. Partitioning of radiotracers between suspended particles and seawater. *Geochim. Cosmochim. Acta.* **48**: 2011–2019.
- MARTIN J. H., AND S. E. FITZWATER. 1988. Iron deficiency limits phytoplankton growth in the north-east Pacific subarctic. *Nature.* **331**: 341–343.
- , AND OTHERS. 1994. Testing the iron hypothesis in ecosystems of the equatorial Pacific Ocean. *Nature* **371**: 123–129.
- , AND R. M. GORDON. 1988. Northeast Pacific iron distributions in relation to phytoplankton productivity. *Deep-Sea Res.* **35**: 177–196.
- MOFFETT, J. W. Transformations among different forms of Fe in seawater. *In* D. Turner and K. Hunter [eds.], *The biogeochemistry of Fe in seawater*. IUPAC Advances in Environmental Chemistry Series. In press.
- PORTER, K. G., AND Y. S. FEIG. 1980. The use of DAPI for identifying and counting aquatic microflora. *Limnol. Oceanogr.* **25**: 943–948.
- PRICE, N. M., AND F. M. M. MOREL. 1998. Biological cycling of iron in the ocean. *Met. Ions. Biol. Syst.* **35**: 1–36.
- RUE, E. L., AND K. W. BRULAND. 1995. Complexation of iron(III) by natural organic ligands in the Central North Pacific as determined by a new competitive ligand equilibration/adsorptive cathodic stripping voltammetric method. *Mar. Chem.* **50**: 117–138.
- SHERR, B. F., E. B. SHERR, AND R. D. FALLON. 1987. Use of monodispersed, fluorescently labeled bacteria to estimate in situ protozoan bacterivory. *Appl. Env. Microbiol.* **53**: 958–965.
- , ———, T. L. Andrew, ———, AND S. Y. Newell. 1986. Trophic interactions between heterotrophic protozoa and bacterioplankton in estuarine water analyzed with selective metabolic inhibitors. *Mar. Ecol. Prog. Ser.* **32**: 169–179.
- VALIELA, I. 1995. *Marine Ecological Processes*. Springer.
- WAITE, T. D., AND F.M.M. MOREL. 1984. Photoreductive dissolution of colloidal iron oxide: Effect of citrate. *J. Colloid. Interface Sci.* **102**: 121–137.
- WELLS, M. L., AND L. M. MAYER. 1991. The photoconversion of colloidal iron hydroxides in seawater. *Deep-Sea Res.* **38**: 1379–1395.
- , ———, O.F.X. Donard, M. M. de Souza Sierra, AND S. Ackleson. 1991. The photolysis of colloidal iron in the oceans. *Nature* **353**: 248–250.
- , N. M. PRICE, AND K. W. BRULAND. 1995. Iron chemistry in seawater and its relationship to phytoplankton: A workshop report. *Mar. Chem.* **48**: 157–182.
- WU, J., AND G. W. LUTHER. 1995. Complexation of Fe(III) by natural organic ligands in the Northwest Atlantic Ocean by a competitive ligand equilibration method and kinetic approach. *Mar. Chem.* **50**: 159–177.

Received: 30 December 1998

Accepted: 10 November 1999

Amended: 18 January 2000